Spectral Sidelobe Regrowth in Saturating Amplifiers

An investigation into the effects of amplifier saturation on spectral sidelobes of digitally-modulated signals

By Frank Amoroso, Consultant, and
Robert A. Monzingo, Raytheon Electronics

Communication systems engineers working in digital data transmission have long been aware of the need for a trade between the prime power efficiency of RF amplifiers and the spectral containment of the data signal produced at the output of those amplifiers. Maximum output power implies maximum prime power efficiency, but not necessarily the best spectral containment. Although the power spectral density of a digital data signal may be well contained by basic bit pulse shaping or by signal pre-filtering at the input of a power amplifier, it remains an axiom of experience that the nonlinear saturating effect of the power amplifier generally tends to cause the spectral sidelobes of the data signal to regrow.

One class of signals that enjoys immunity from the regrowth effect [1] is the constant carrier envelope signal, such as minimum shift keying (MSK) or other forms [2] of digital frequency shift keying (FSK). Classical MSK, unfortunately, lacks the inherent spectral containment [1] required in the regulatory environment of modern wireless communications, and the spectrally contained forms of FSK, such as [3] Gaussian Minimum Shift Keying (GMSK), require rather complex detection schemes to deliver maximum communications efficiency.

Of considerable interest for its simplicity of implementation [4] is the offset quadrature phase shift keyed (OQPSK) modulation format, which includes both classical MSK and the more spectrally contained versions that use root raised cosine (RRC) data pulses [5] or quasi-bandlimited (QBL) data pulses [6,7]. The latter class of pulses is distinguished by the relatively small ripple that results in the radio frequency carrier magnitude at the power amplifier input. Minimization of ripple is a design goal, for the less carrier ripple, the better the signal's power spectral density resists sidelobe regrowth under saturation conditions.

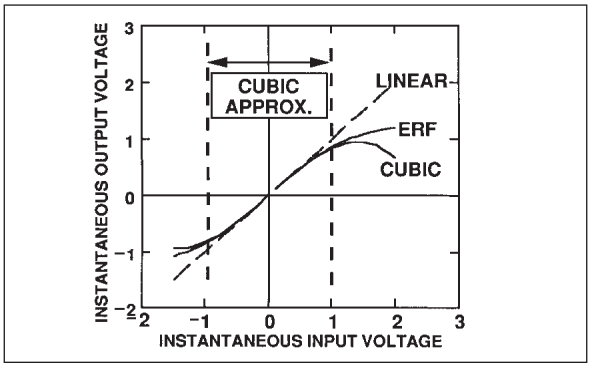

■ **Figure 1. Nonlinear transfer characteristic.**

This article describes the details of the process by which spectral sidelobes regrow as amplifier drive level is increased. It provides insight into the dependence of sidelobe regrowth on the details of carrier ripple, and the rate at which spectral sidelobes regrow as the amplifier drive level is increased.

It will be seen that the dependence of sidelobe power level on amplifier drive level is virtually the same for all well-designed signals, but the exact shape of regrown sidelobes depends very much on the precise details of the signal. A new signal form, called the "para-signal," will be derived simply and abstractly from the undistorted data signal as it appears at the power amplifier input. The para-signal uniquely sets the shape of the regrown spectral sidelobes.

Signal and amplifier definitions

As has been customary [8,9], the saturating amplifier is modeled as an odd-symmetric memoryless nonlinearity followed by a zonal bandpass filter. (The phenomenon of AM/PM conver-

sion has been set aside for this introductory discussion.) The nonlinearity is shown in Figure 1 in two different forms. The form labeled "ERF" is the nonlinearity actually contained in the amplifier

$$V_{out}(t) = \sqrt{\frac{\pi}{2}} erf\left[\frac{V_{in}}{\sqrt{2}}\right] \quad (1)$$

(There are many forms of the erf function in circulation. The form shown here is that used in the Mathcad computer application by Mathsoft, Inc.,)

This saturation characteristic has been recommended by several authors [10,11]. In Figure 1, the form marked "CUBIC" is a two term Taylor's series approximation to (1), ending with the cubic term, as given by

$$V_{out}(t) = K_1 V_{in}(t) + K_3\left[V_{in}(t)\right]^3 \quad (2)$$

The analysis of sidelobe regrowth is greatly facilitated by the cubic approximation in (2), and that approximation holds for input voltages up to roughly 1 volt. In (2), the constant K_1 associated with the linear term is assumed normalized to unity without loss of generality. In Figure 1, the reference line marked "LINEAR" has unit slope and is tangent to the saturation characteristic. The value of K_3 for the nonlinear characteristic of (1) is readily computed to be –1/6.

The data modulation is OQPSK operating at a net rate of 1/T bits per second, comprising the in-phase (I) and quadrature (Q) data channels. The bit rate on each of the I and Q channels is therefore 1/2T bits per second. The basic data pulse for both the I and Q channels is the "trapezoidal" pulse drawn from the same pulse class as previously discussed [6,7] in connection with the hard limiting of signals

$$p(t) = \frac{\sin\frac{\pi}{2T}t}{\frac{\pi}{2T}t} \times \frac{\sin\frac{\pi}{4T}t}{\frac{\pi}{4T}t} \quad (3)$$

where the descriptor "trapezoidal" refers to the shape of the Fourier transform of the pulse as shown in Figure 2a. If the pulse were allowed to extend from time –∞ to +∞, then its Fourier transform would be a trapezoid, but in practice some time truncation is dictated. For the present study, the pulse is truncated to the time interval (–4T, +4T) to facilitate spectrum calibrations [12]. It is also subjected to windowing [13], sometimes called tapering, to reduce the time truncation sidelobes and thereby expose the sidelobe regrowth to clearer view.

The spectrum of the truncated but unwindowed pulse is shown as the dashed line in Figure 2b, and the spectrum of the truncated windowed pulse is the lower solid curve in Figure 2b. With random data and linear amplification up to the power amplifier input, the spectrum of $s(t)$ takes the same form as the spectrum of an isolated $p(t)$. Clearly, the spectral sidelobes of $p(t)$, and therefore of the linearly amplified $s(t)$, are quite low. The spectrum of the hard limited signal is shown as the upper solid

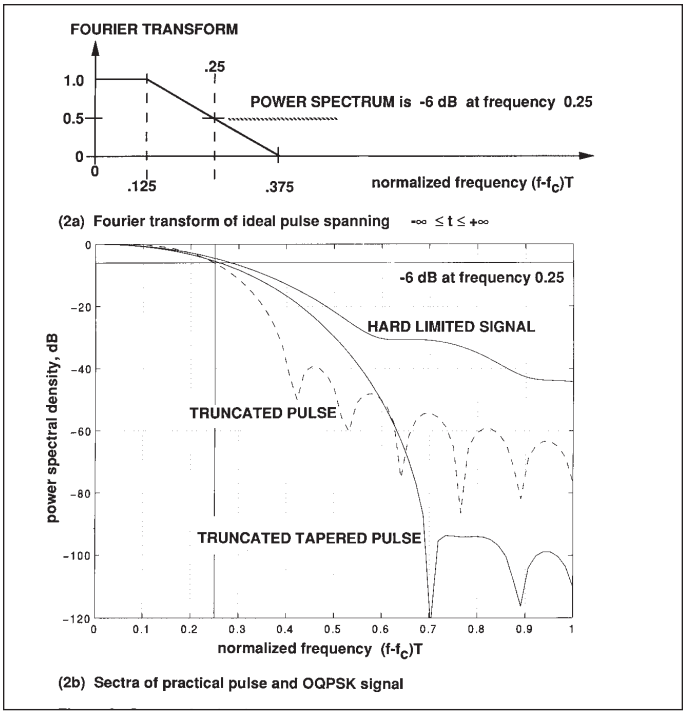

■ **Figure 2. Spectra for data signals, all normalized to 0 dB at $(f–f_c)T=0$. The truncated tapered pulse spectrum in (2b) is the actual signal spectrum for very small amplifier input power level.**

curve in Figure 2b. The amplifier output at moderate drive levels will exhibit sidelobe regrowth that brings the spectrum to various intermediate levels between the two solid curves in Figure 2b. Those spectra will be shown and discussed shortly.

It is useful to note that Figures 2a and 2b are quantitatively linked by the ordinate value at frequency $(f-f_c)T=0.25$ that is common to both figures. In Figure 2a, the Fourier transform has dropped from unity to the value 0.5 at frequency 0.25, which means that the pulse spectrum has dropped to –6 dB. In Figure 2b, all three plotted spectra are –6 dB at frequency 0.25, which confirms the commonality of nominal bandwidth among the four different versions of the signal spectrum.

For analysis of spectral regrowth, the composite data signal entering the power amplifier will be expressed in the usual [2] complex baseband form.

$$s(t) = \alpha(t)e^{j\emptyset(t)} \quad (4)$$

where α is the carrier magnitude and $e^{j\emptyset(t)}$ is the phase modulation. A further useful step of manipulation, not found in previous analysis, is to express $\alpha(t)$ as the product of the mean magnitude α_o times the sum of unity and a ripple component $\delta(t)$

$$\alpha(t) = \alpha_o\left[1+\delta(t)\right] \quad (5)$$

so that $s(t)$ becomes

$$s(t) = \alpha_o\left[1 + \delta(t)\right]e^{j\emptyset(t)} \tag{6}$$

Spectral analysis

After some further manipulation [12], the bandpass signal at the output of the power amplifier, based on the approximation in (2), becomes

$$\begin{aligned} r(t) &= \left(1 + 0.75K_3\alpha_o^2\right)s(t) + 1.5K_3\alpha_o^3\delta(t)e^{j\emptyset(t)} \\ &= \left(1 - \frac{\alpha_o^2}{8}\right)s(t) - \frac{\alpha_o^3}{4}\delta(t)e^{j\emptyset(t)} \end{aligned} \tag{7}$$

where α_o now measures the amplifier input drive level.

The first term on the right side of (7) shows that as the drive level is increased the (initially unity) gain of the amplifier is decreased by the amount $\alpha^2_o/8$. The second term on the right of (7) shows that, in addition to $s(t)$, a second type of signal enters with amplitude $\alpha_o^3/4$. That new signal type is now defined as the "para-signal"

$$\Delta(t) = \delta(t)e^{j\emptyset(t)} \tag{8}$$

The first para-signal factor $\delta(t)$ goes positive and negative as the rippling RF carrier magnitude of $s(t)$ goes above and below its mean value. Of course, the second para-signal factor $e^{j\emptyset(t)}$ presents unit magnitude and is indistinguishable from a bandpass hard limited version of $s(t)$ with the limiter output magnitude set to unity.

One significance of the para-signal $\Delta(t)$ is obvious on inspection of (7). If the magnitude of $s(t)$ is constant, then $\delta(t)$ is null everywhere and the amplifier output is simply a linearly scaled representation of $s(t)$. There is no spectral sidelobe regrowth, although the gain of the amplifier drops off as saturation occurs. Evidently, then, $\Delta(t)$ via (7) represents the spectral sidelobe regrowth term in some significant sense, to be explored shortly.

Although the amplifier input signal amplitude is proportional to α_o, the amplitude of the para-signal component $\Delta(t)$ in (7) is proportional to α_o^3. This implies that the rate growth of the spectral sidelobes will be three times as great, when measured in decibels, as the rate of growth of the drive level α_o. This phenomenon is remarkably reminiscent of the rate of growth of third order intermodulation products in saturating amplifiers [8, 9] driven by a two-tone signal. Recall that the power level of third order intermodulation products grows three times as fast as the power level of the input tones.

Amplifier output spectra

Figure 3 shows the amplifier output spectra for drive levels α_o=0.2, 0.4 and 0.8, which are all within the range

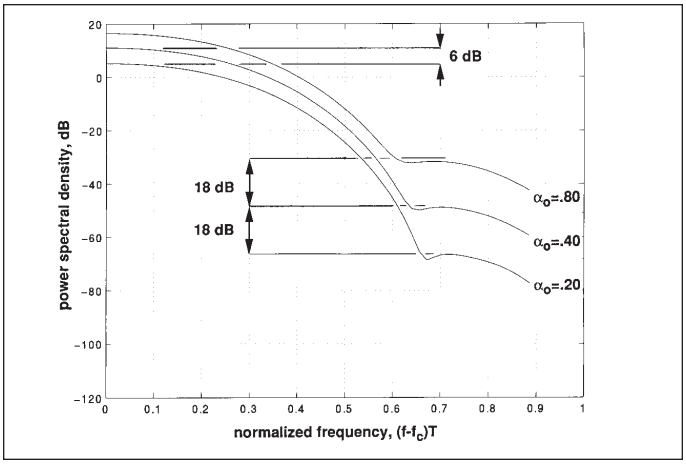

■ **Figure 3. Power amplifier output spectra for three drive levels 6 dB apart.**

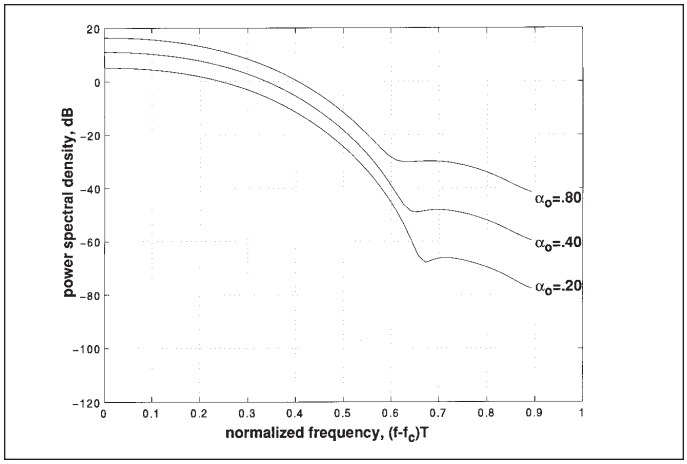

■ **Figure 4. Estimated power amplifier output spectra for three drive levels 6 dB apart, based on cubic approximiation to amplifier nonlinearity.**

of applicability of both the assumed nonlinear characteristic of (1) and the Taylor's series approximation of (2). The spectra of Figure 3 are based on (1). They validate the conclusion inferred from (7), i.e., as the drive level increases in steps of 6 dB, the spectral sidelobes increase in steps of 18 dB. The shapes of the three spectra in Figure 3 are nearly identical for the plotted frequency range, confirming that there is a single functional process underlying sidelobe regrowth over a wide range of drive levels.

The precision of the cubic approximation to the nonlinear characteristic is tested next in Figure 4, which is based explicitly on the r(t) of (7) for the same set of drive levels used in Figure 3. The spectra in Figure 4 coincide

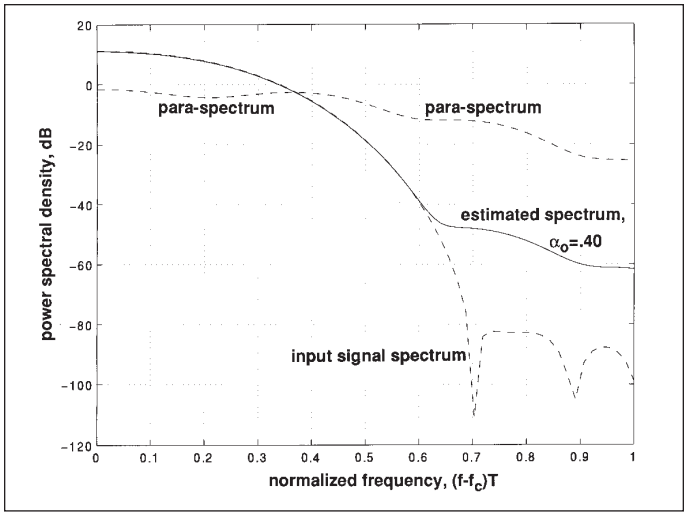

■ **Figure 5. Estimated power amplifier output spectrum for α_0= 0.40, based on the sum of input signal spectrum and para-spectrum.**

well with those of Figure 3 up to frequency $(f–f_c)T=0.9$, which includes that portion of the spectrum that normally figures critically in compliance with regulatory bounds on power spectral density. The frequency 0.9 is already 3.6 times the nominal Nyquist signal bandwidth of 0.25, and as long as the spectrum continues to drop off beyond that point, the discrepancies between Figures 3 and 4 are not highly consequential.

Figure 5 deals with the most speculative and most intriguing aspect of equation (7). The lower dashed curve shows, for α_o= 0.4, the spectrum of $(1–\alpha_o^2/8)s(t)$. The upper dashed curve shows the power spectrum of $\Delta(t)$ normalized to 0 dB at zero frequency. The solid curve is the sum of the two component spectra shown in the dashed curves, with the spectrum of $\Delta(t)$ scaled according to (7). The solid curve then represents the sum of the spectra of the two terms on the right side of (7).

Comparison of Figure 5 with Figure 4 shows that the amplifier output spectrum, with the ERF nonlinearity, is accounted for over almost the entire frequency range by a simple summing of the properly weighted para-spectrum [i.e., the power spectral density of $\Delta(t)$] with the properly weighted $s(t)$ spectrum. The only visible discrepancy (about 2 dB) between Figure 5 and Figure 4 occurs over a rather small frequency interval, around $(f–f_c)T=0.65$.

This small discrepancy might be accounted for by the fact that the spectrum of the r(t) of (7) is, strictly, the Fourier transform of the *autocorrelation function* of r(t). If $s(t)$ and $\Delta(t)$ are statistically correlated, then the autocorrelation function of r(t) is considerably more complex that just the weighted sum of the spectra of $s(t)$ and $\Delta(t)$ taken individually. Indeed, in the examples treated thus far, there does appear to be about a 20 percent correlation between $s(t)$ and $\Delta(t)$. Therefore, the role of the para-spectrum in the spectral sidelobe regrowth process remains the subject of continuing investigation. ■

References

1. F. Amoroso, "The Bandwidth of Digital Data Signals," *IEEE Communications Magazine*, Vol. 18, No. 6, November 1980, pp 13-24.

2. J.G. Proakis, *Digital Communications*. New York: McGraw-Hill, 1983.

3. K. Hirade and K. Murota, "GMSK modulation for digital mobile radio telephony," *IEEE Transactions on Communications*, Vol. COM-29, No. 7, July 1981, pp 1044-1050.

4. F. Amoroso and J.A. Kivett, "Simplified MSK Signaling Technique," *IEEE Trans. on Comm.*, Vol. 25, No. 4, April 1977, pp 433-441.

5. S. Chennakeshu and G.J. Saulnier, "Differential detection of π/4-shifted DQPSK for digital cellular radio," *IEEE Transactions on Vehicular Technology*, Vol. 42, No. 1, February 1993, pp 46-57.

6. F. Amoroso, "The use of Quasi-Bandlimited Pulses in MSK Transmission," *IEEE Trans. on Comm.*, Vol. COM-27, No. 10, October 1979, pp 1616-1624.

7. F. Amoroso and M. Montagnana, "Distortionless Data Transmission with Minimum Peak Voltage," *IEEE Transactions on Information Theory*, Vol. IT-13, No. 3, July 1967, pp 470-477.

8. B. Gallagher, "Estimating and measuring C/I in a GSM wireless local loop receiver," *Microwave Journal*, Vol. 40, No. 10, October 1997, p 70 ff.

9. F.C. McKay, "Don't guess the spurious level," *Electronic Design* 3, February 1, 1967, p 70 ff.

10. J.J. Spilker, *Digital Communications by Satellite*, Englewood Cliffs: Prentice-Hall, 1977.

11. R.M. Gagliardi, *Satellite Communications*, New York: Van Nostrand, 1984.

12. F. Amoroso and R.A. Monzingo, "Analysis of data spectral regrowth from nonlinear amplification," *1997 IEEE International Conference on Personal Wireless Communications* (ICPWC '97), Mumbai (formerly Bombay), India, Dec. 17-20, 1997, pp 142-146. (Reprints available from authors.)

13. F. Harris, "On the use of windows for harmonic analysis with the discrete Fourier transform," *Proceedings of the IEEE*, Vol. 66, No. 1, January 1978, pp 19-51.

Author information

Frank Amoroso received BS and MS degrees in electrical engineering from MIT and has pursued further graduate studies at Purdue University and the University of Turin, Italy. He is a private consultant to a number of industrial firms and is based in Santa Ana, CA. He may be reached by phone or fax at (714) 557-1061.

■ **Amoroso.**

Robert A. Monzingo received a ScD degree in systems and automatic control from Washington University in St. Louis, MO. He is a senior scientist in the Adaptive & Signal Processing Systems Group of Raytheon Electronics in Los Angeles, CA. He may be reached by phone at (310) 334-2492, by fax at (310) 607-1559 and by e-mail at ramonzingo@ccgate.hac.com.

■ **Monzingo.**